A Programmable Array for Contact-Free Manipulation of Floating Droplets on Featureless Substrates by the Modulation of Surface Tension

Amar S. Basu and Yogesh B. Gianchandani

***Abstract*—This paper presents a contactless droplet manipulation system that relies on thermally generated Marangoni flows. Programmable 2-D control of aqueous microdroplets suspended in an oil film on a plain featureless glass substrate is achieved using a 128-pixel heater array suspended 100–500 μm above the oil layer. The heaters generate surface temperature perturbations (< 25 °C), resulting in local Marangoni flows that can move droplets in either a push or a pull mode. Programmed movement is achieved by the sequential activation of the heaters, with digital control circuitry and a graphical interface providing addressable control of each heater. Droplets with diameters of 300–1000 μm are manipulated and merged at speeds up to 140 μm/s. Evaporation rates can be reduced by almost two orders of magnitude by using a two-layer-oil medium, and the choice of an optimum carrier fluid can achieve fluid velocities over 17 000 μm/s. The system provides a contactless platform for parallel droplet-based assays. As such, it circumvents the challenges of sample contamination and loss that occur when a droplet interacts with a solid surface. [2008-0272]**

***Index Terms*—Droplet, fluid-flow control, Marangoni flow, programmable microfluids, thermal.**

I. Introduction

MICROFLUIDIC actuators often exploit physical phenomena that are enhanced at small length scales [1], [2]. Specifically, laminar flows and the high surface-area-to-volume ratio that are present in microfluidic devices enable many pumping techniques that rely on surface interactions. Electrowetting [3] and electroosmosis [4], for example, both rely on the movement of electrical charges at a liquid–solid interface to create plug flow in a channel or the movement of droplets along a 2-D grid of electrodes. Gradients in the chemical surface energy at the solid–liquid contact line can also be used to propel droplets across surfaces [5].

Manuscript received November 2, 2008; revised June 25, 2009. First published September 29, 2009; current version published December 1, 2009. This work was supported in part by the National Science Foundation and in part by the University of Michigan. The work of A. S. Basu was supported by a Whitaker Foundation Biomedical Engineering Fellowship. The work of Y. B. Gianchandani was supported by the Independent Research/Development Program while he was with the National Science Foundation. The findings do not necessarily reflect the views of the NSF. Subject Editor C. Mastrangelo.

A. S. Basu is with the Department of Electrical Engineering and Computer Science, University of Michigan, Ann Arbor, MI 48109-2122 USA, and also with the Department of Electrical and Computer Engineering, Wayne State University, Detroit, MI 48202 USA.

Y. B. Gianchandani is with the Department of Electrical Engineering and Computer Science, University of Michigan, Ann Arbor, MI 48109-2122 USA.

Color versions of one or more of the figures in this paper are available online at http://ieeexplore.ieee.org.

Digital Object Identifier 10.1109/JMEMS.2009.2029961

Thermocapillary (Marangoni) flow, which is the flow of liquids due to surface-tension gradients at a liquid–air interface, is another phenomenon that is suitable for microfluidic actuation. Past approaches for exploiting Marangoni flow have used temperature gradients generated on a planar substrate patterned with heaters. For example, a gradient imposed across a microfluidic channel can move droplets in the channel via a "thermowetting" phenomenon [6], [2]. The same effect was shown to create fingering instabilities in thin liquid films [7]. Stroock *et al.* [8] demonstrated directional Marangoni flow on a uniformly heated chip that contained ratchetlike structures to rectify the flow.

Instead of using a fluidic substrate to generate temperature gradients, Marangoni flow can also be generated by imposing a temperature gradient on the surface of the liquid layer. This approach circumvents the need for patterned substrates and enables the formation of sharp temperature profiles due to the low thermal conductivity of air. In past efforts, a *steady-state* heat source of customized shape was suspended in air just above the fluid surface. The shape of the heat source determined the nature of the flow pattern [9]. Using simple geometries such as lines, rings, and tapered shapes, we have previously demonstrated numerous Marangoni flows for droplet mixing and control [10], [11]. However, for greater flexibility and dynamic reconfigurability, the question still remains whether a regular array of miniature heaters can be operated under dynamic control to provide fluidic manipulation on a featureless substrate. This effort[1] describes a way to generate programmable heat fluxes using a 2-D grid of heaters suspended above the fluid layer.

One potential application of the system is the manipulation of microdroplets. Digital microfluidic systems use aqueous droplets suspended in an immiscible phase to encapsulate reagents and serve as reaction containers. Precise user-defined chemical reactions may be achieved by transporting and merging droplets containing the appropriate samples and reagents [13]. Compared to traditional microfluidics where samples are flowed through microchannels, digital microfluidics provides an elegant approach to high-throughput assays, offering inherent encapsulation, low reagent consumption, and fast reaction times. Programmable fluidic processors refer to systems that can dynamically control the movement of droplets [14], [15] in a 2-D space using methods such as electrowetting-on-dielectric

[1]Portions of this paper have appeared in conference abstract form in [12].

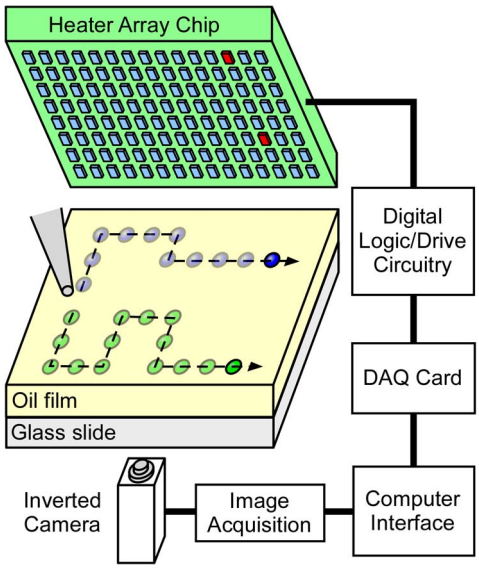

Fig. 1. Complete system for programmable noncontact droplet actuation based on Marangoni flows, including a 128-pixel array of resistive heaters suspended above the oil layer, a control circuitry, and a graphical user interface.

[3], optoelectrowetting [16], dielectrophoresis [14], and magnetic fields [17].

The system described in this paper provides a complementary approach to droplet manipulation whereby Marangoni flows generated in an oil layer are used to manipulate the droplets (Fig. 1). Local Marangoni flows can be initiated by activating heater pixels in the array, and droplet movement can be achieved through the sequential activation of adjacent heaters. Two contributions of this approach are as follows: 1) it circumvents the need for complex substrates, and 2) it does not require physical contact with the droplet, which can alleviate problems related to adsorption [13], [18], [19].

Section II provides a theoretical basis and simulations of push- and pull-mode actuation. Section III details the system design and experimental setup, and Section IV provides experimental results. Section V discusses experimental considerations, provides an argument for scaling down the size of the system, and compares this approach with existing methods for droplet manipulation. Section VI gives conclusions.

II. Theoretical Modeling

Local Marangoni flows can be initiated on the free surface of a liquid layer by placing a millimeter-scale heat source above the surface and in close proximity to it (i.e., typically < 1 mm away). Heat transfer through the air gap increases the surface temperature of the liquid immediately beneath the heat source and creates a radial temperature gradient. In most liquids, surface tension is inversely related to temperature; thus, the temperature gradient creates an inverse gradient in surface tension. This results in a shear stress (τ_s) at the liquid interface given by the following boundary condition [9], [20]:

$$\tau_s = \mu \frac{d\vec{u}_S}{d\vec{N}} = -\sigma_T \nabla T_S \tag{1}$$

where μ is the liquid viscosity, σ_T is the surface-tension temperature coefficient, ∇T_S is the surface-temperature gradient,

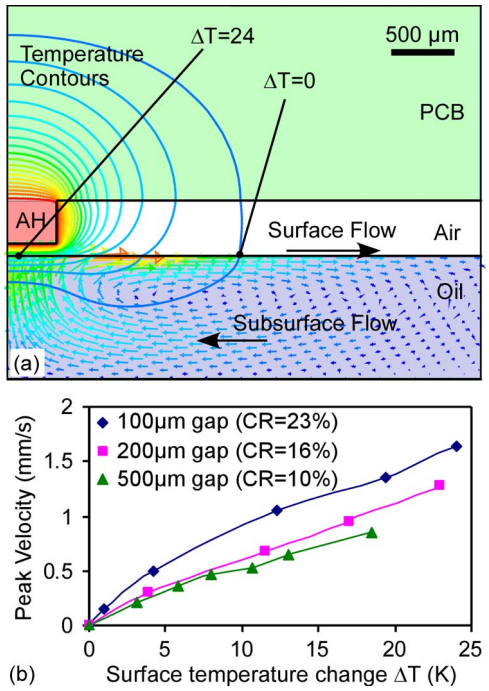

Fig. 2. Results from a CFD simulation (FLUENT 6.0). (a) Surface-temperature contours generated by an active heater and velocity vectors of the surface and subsurface Marangoni flows. AH denotes the alumina heater. (b) Flow velocity versus peak surface-temperature change for 100-, 200-, and 500-μm gaps between the heater and the liquid. CR represents the coupling ratio, which is defined as the ΔT on the liquid surface divided by the ΔT in the heater.

$\vec{u}_S$ is the tangential surface velocity, and $\vec{N}$ is the surface normal vector. The resulting surface Marangoni flow $(\vec{u}_S)$ is directed away from the heat source, and it is accompanied by subsurface flows oriented in the opposite direction. The flow region extends radially from beneath the heat source, and its radius increases with the thickness of the oil layer. Typical values are 120 μm in a 100-μm-thick oil layer up to nearly 1150 μm in a 380-μm-thick layer [10], [11]. Due to viscous shear, velocities tend to decrease when the oil-layer thickness is < 200 μm. By tuning the geometry of the temperature profile imposed on the liquid surface, a variety of recirculating Marangoni flows can be created. As indicated earlier, this was previously done by using steady-state heat sources of various geometries suspended above the fluid layer [10], [11].

The more generalized approach, which is the subject of this paper, utilizes a 2-D array of heaters to achieve spatiotemporal control of the surface-temperature profile and obtain dynamically controlled droplet movement. Each heater, when activated, creates a local temperature gradient on the liquid surface, which results in surface and subsurface Marangoni flows [see the simulation, Fig. 2]. The heater can either push a droplet away with its surface flow or pull a droplet toward it via its subsurface flow, depending on the size of the droplet and the depth of the flow region. For the purposes of this paper, the former is labeled push-mode actuation, while the latter is labeled pull-mode actuation. Droplet movement in both modes can be controlled through the sequential activation of individual heaters.

TABLE I
MATERIAL PROPERTIES FOR THREE LIQUIDS USED IN GENERATING MARANGONI FLOWS. VALUES MARKED WITH AN * ARE CALCULATED USING THE EÖTVÖS LAW, AND THOSE MARKED WITH ** ARE ESTIMATED FROM SIMILAR FLUIDS

			Liquid			
Parameter	Symbol	Units	Mineral Oil USP	DC550 Silicone oil	DC704 Silicone oil	Fluorinert™ FC-3283 dielectric liquid
Density	ρ	kg/m^3	886	1070	1070	1820
Surface tension coefficient	σ_T	mN/m-K	-0.220	-0.069**	-0.036 *	-0.410 *
Thermal Conductivity	κ	W/m-K	0.12	0.1463	0.16 **	0.066
Viscosity	μ	kg/m-s	0.026	0.134	0.042	0.0014
Figure of Merit	$\lvert\sigma_T/\kappa\mu\rvert$		$7.1x10^{-2}$	$3.5x10^{-3}$	$5.3x10^{-3}$	4.44
References			[6], [26]	[27], [30]	[28], [26]	[25]

A. Push- and Pull-Mode Actuations

Both push- and pull-mode actuations can be evaluated by computational fluid dynamics (CFD) software (FLUENT 6.0, Fluent Corporation). The software uses an iterative procedure to compute the coupled thermal–fluid problem. In each iteration, it solves the energy equation, equates the surface-temperature gradient to a shear stress using eq. (1), and then calculates the flow in the liquid layer using the continuity and Navier Stokes equations. The process repeats until all sets of equations converge.

Fig. 2 shows the temperature contours and flow vectors generated by a resistive heater held 100 μm above a layer of silicone oil. The heater consists of an 800-μm-wide surface-mount chip resistor on a printed circuit board (PCB). The problem is modeled in a 2-D axisymmetric geometry. A heat-generation boundary condition is applied to the surface of the chip in order to tune the temperature of the heat source to the desired temperature. The thermal conductivities of the alumina chip and PCB are 27.6 and 0.3 W/m · K, respectively, and the liquid is assumed to be DC-550 silicone oil (Dow Corning, Midland, MI), with the properties being listed in Table I. In the example shown in Fig. 2(a), the increase in fluid temperature is 24 °C, and the outward temperature gradient results in a flow velocity of 1.6 mm/s.

Simulations over a range of heat input conditions [Fig. 2(b)] indicate that the flow velocity is proportional to the temperature gradient imposed on the liquid surface. The temperature gradient, in turn, is proportional to the following: 1) the heater temperature and 2) the thermal coupling between the heat source and the liquid surface. Due to the low thermal conductivity of air, the thermal coupling between the heater and the liquid is strongly dependent on the separation gap. For example, at a 100-μm separation, the temperature increase at the liquid surface (i.e., the coupling ratio) is 23% of the temperature increase in the heat source. At a 500-μm gap, the coupling ratio falls to 10%. Another important requirement for sharp lateral temperature gradients is the use of suspended heaters rather than heaters embedded in the liquid. If the heaters are embedded in the liquid, the comparatively high thermal conductivity of the liquid (about five times higher than air) would limit the formation of sharp gradients and thereby reduce the velocity of Marangoni flow. Furthermore, it would cause undesirable heating in the liquid.

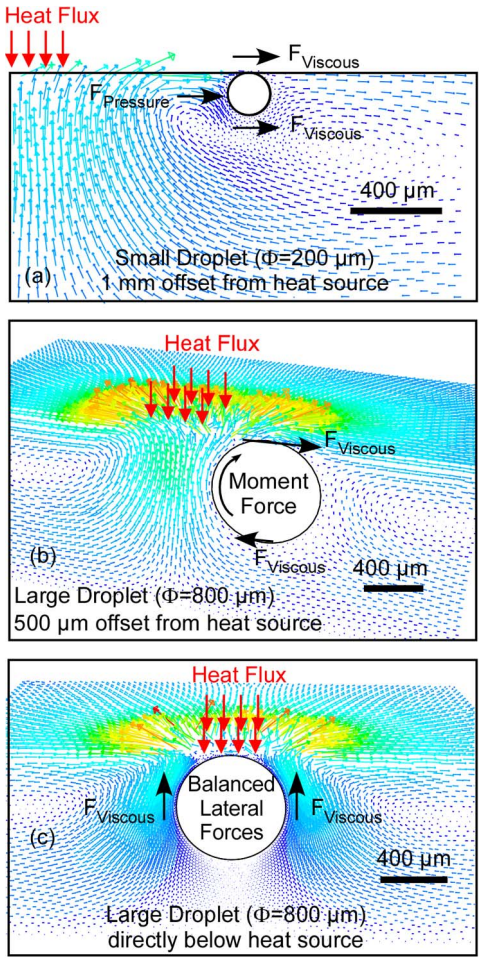

Fig. 3. Three-dimensional CFD simulation of push- and pull-mode actuations on $\Phi = 200$-μm and $\Phi = 800$-μm droplets, respectively. The droplet volumes were meshed as an immiscible spherical volume within the fluid layer. (a) Flow vectors showing pressure and viscous forces on a 200-μm droplet that is offset 1 mm from the center of the heat source. (b) Moment force on an 800-μm droplet that is offset 500 μm from the center of the heat source. (c) A trapped 800-μm droplet after it has been pulled into the center of the heat source.

The interaction of droplets with the flow is shown in Fig. 3. This set of simulations includes a 3-D fluid layer with an embedded spherical volume to represent the immiscible droplet. The droplet is positioned such that its upper surface is in contact with the top of the oil layer but does not protrude above the surface. This geometry is consistent with empirical observations of a droplet dispensed in the oil layer. It is believed that interfacial forces at the surface of the oil layer form a skin that holds the droplet below the surface, and the thin layer of oil separating the droplet from the air allows the shear force in the oil to be coupled to the droplet. Observations also indicate that the buoyant force on the droplet is not strong enough to deform its shape. A surface heat flux of 50 mW/mm^2 is added to a 1-mm square region in the center of the fluid layer to model the local heating (indicated by the arrows). Assuming the properties of DC-550 fluid, this results in a recirculating flow (maximum surface-flow velocity of 6 mm/s) that applies pressure and viscous forces to a droplet. The lateral pressure and viscous forces on the droplet are calculated by integrating the respective forces along the surface area of the droplet. Moment forces are integrated in a similar manner using the droplet centroid as the axis. Fig. 3 shows simulated forces in the push and pull modes of operation, depending on the size of the droplet. A droplet that is < 200 μm in diameter [Fig. 3(a)] gets pushed away from the active heater by surface flows (push mode). In this case, the droplet's center of mass is near the fluid surface, which is dominated by outward-directed surface Marangoni flows. A combination of pressure and viscous forces pushes the droplet outward. In contrast, a larger droplet (for example, $\Phi = 800$ μm) tends to get pulled in toward the active heater [Fig. 3(b)]. In this case, the droplet's center of mass is deeper below the surface, where the inward-directed subsurface flows are more significant. It is also interesting to note that the opposing surface and subsurface flows create a *moment* force on the droplet, which causes the droplet to rotate, as observed in experiments. It is believed that the spinning motion, along with the buoyant force, helps to "roll" the droplet toward the center. Once at the center, the droplet is stabilized by the balanced forces on either end of the droplet [Fig. 3(c)]. A quantitative comparison of the moment and body forces on large ($\Phi = 800$-μm) and small ($\Phi = 200$-μm) droplets is shown in Fig. 4. The large droplet clearly experiences a moment force at a distance of 500 μm from the center, while the small droplet experiences virtually no moment force. The large droplet also experiences a radial force (up to 0.6 μN), but unlike the small droplet, the force is directed toward the heat source rather than away from it. In summary, droplet movement in both push and pull modes is driven by viscous and pressure forces imparted by the thermally generated Marangoni flows. Due to the relatively small inertial forces at millimeter and micrometer length scales, droplets in the flow respond without latency to changes in flow velocity.

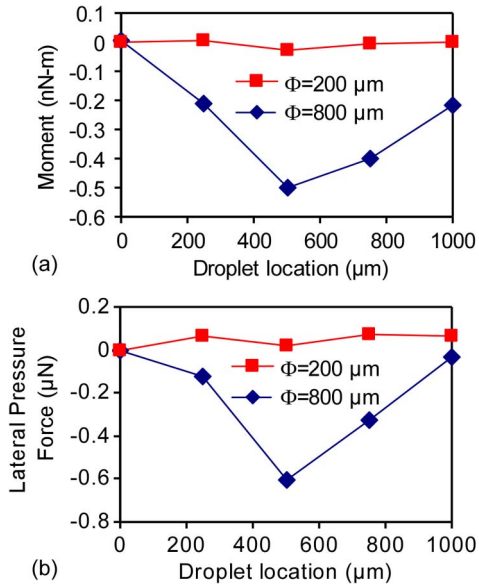

Fig. 4. Simulated results. Forces acting on $\Phi = 800$-μm and $\Phi = 200$-μm droplets, which are taken from the simulation in Fig. 3. (a) Moment force on the two sizes of droplets at various lateral offset distances from the center of the heat source. (b) Radial force (directed away from the heat source) for the two droplets, also at various distances from the heat source.

B. Choice of Fluid

Several aspects must be considered when choosing an appropriate carrier fluid in which to create the Marangoni flows. First and foremost, the oil should be chosen to maximize coupling between flow speed and applied heat. To represent this criteria, a figure of merit may be used. Equation (1) implies that, under a given temperature gradient, the Marangoni flow velocity is proportional to σ_T/μ. The gradient itself is inversely proportional to thermal conductivity κ. Therefore, the figure of merit for a given fluid is

$$FOM = -\frac{\sigma_T}{\mu\kappa}. \tag{2}$$

Fluid density is not included in this FOM because natural convection is not significant in thin layers of fluid [20]. Surface-tension coefficients are seldom provided for most chemicals, but they can be estimated using the Eötvös law $\sigma_T = k_\gamma / V_m^{2/3}$, where V_m is the molar volume of the liquid and $k_\gamma = 2.1 \times 10^{-7}$ J/K for virtually all liquids [21], [22]. They can also be experimentally measured using the DeNouy ring method or drop-shape analysis. Over the range of carrier fluids examined in this paper, the surface-tension coefficients do not vary by more than two to five fold. Thermal-conductivity data for fluids is generally available. Aqueous films, for example, have relatively high thermal conductance (0.6 W/m · K), which limits the formation of sharp surface-temperature gradients. In contrast, typical mineral and silicone oils have conductivities that are only 20% that of water and also have fairly low vapor pressures to reduce evaporative effects. Fluorinated organic liquids, with thermal conductivities that are one order of magnitude less than that of water, function as excellent carrier fluids for Marangoni flows. However, their evaporation rates are somewhat higher than that of mineral oils. The FOM for a given liquid predicts the velocity of Marangoni flow generated in the bulk oil layer.

When a droplet is introduced, the interactions of the fluid with the droplet must also be considered. First, the fluid must be hydrophobic so that the water droplets within it are immiscible

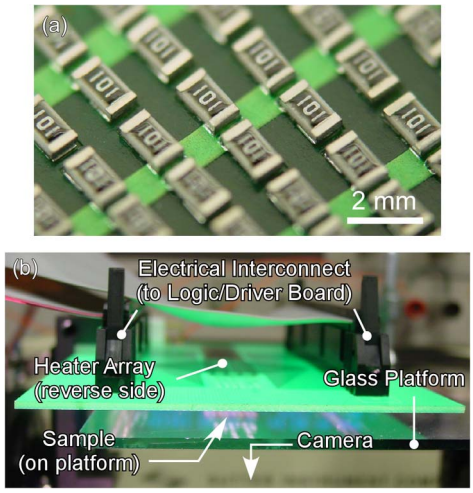

Fig. 5. (a) Micrograph of the heater array. (b) Experimental setup. The heater array is mounted on the lower side of a PCB, facing the sample, which is placed on a glass platform. The droplet movement is imaged by an inverted CCD camera mounted below the platform (not shown in the photograph).

and biocompatible to allow for biomolecular reagents. Second, the fluid should have a higher density than water, which ensures that the droplets float on top of the oil layer and do not drag or adhere to the glass substrate below. Empirical evidence shows that the buoyant force exerted on the droplet does not have a significant impact on coupling flow to droplet movement. Last, the liquid should be of low volatility to prevent undesired evaporation.

Given the diverse set of requirements, three oils were chosen. The first is mineral oil (USP, Rite Aid Pharmacy), a biocompatible transparent oil that is often used in biochemical assays for reagent encapsulation (for example, to encapsulate embryos and in high-throughput screening assays). This oil is less dense than water, so it is used primarily for characterization and for particle experiments. The second group of fluids includes high-density silicone oils, such as DC-550 and DC-709 (Dow Corning), which allow the droplets to float on the surface. The last fluid is Fluorinert (FC-3283, 3M Corporation), a fully fluorinated dielectric fluid that has very low thermal conductivity, low miscibility to water, and high density. FC-3283 has often been used as a carrier fluid in microdroplet systems [13]. Material properties for each of these fluids are given in Table I.

III. System Design and Experimental Setup

The 16×8 heater array used to initiate Marangoni flow consists of #0603 surface-mount resistors ($1 \times 0.8 \times 0.3\ \text{mm}^3$) placed at 1.9-mm pitch on a two-sided PCB (Fig. 5). The 100-Ω resistors are electrically connected via through-holes to the opposite side of the PCB which provides routing, cable connectors, and a heat sink. The two-sided design allows the resistors to be placed near the liquid without obstruction. Commercial foundries are used to manufacture PCBs (Sunstone Circuits, Mulino, OR) and to assemble the resistors in a solder reflow process (Screaming Circuits, Canby, OR).

A separate PCB houses the addressing logic and driver circuitry, with electrical interconnect being provided by two 64-pin ribbon cables. A bank of power DMOS transistors, one

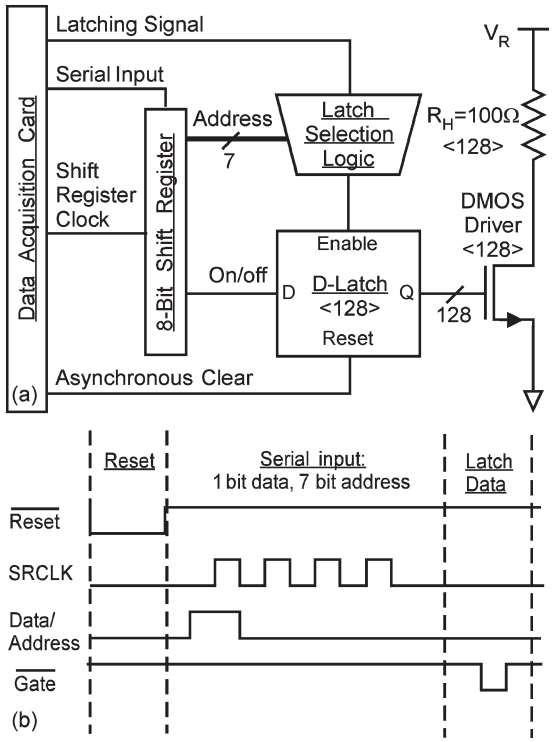

Fig. 6. (a) Schematic of logic and driver electronics. There are 128-Joule heaters and one D-latch and driver for each (these elements are represented by $\langle 128 \rangle$). The remaining components are shared. The forward slash indicates a multiline bus, and the number beneath indicates the number of lines on the bus. (b) Timing diagram showing the serial input scheme for toggling heaters on and off.

for each resistor, can provide a maximum of 250-mA current, or 6.25-W power, to each heater [Fig. 6(a)]. The range of power actually used is much smaller, which is typically < 1.3 W. The heater power is set globally for all the resistors by adjusting the voltage V_R, with typical voltages ranging from 8 to 12 V.

Heaters are individually set and reset via a graphical interface and control circuitry. D-latches are used to maintain the ON/OFF state of each heater. A PCMCIA digital I/O card (NI-6062E, National Instruments) connected to a laptop computer toggles the state of each heater using a four-line serial protocol [Fig. 6(b)]. The *shift-register clock* signal synchronizes the loading of a command sent via *serial input* line into the shift register. During the first eight clock cycles, the shift register is loaded with 7 bits indicating the address of the resistor and 1 bit signifying an ON or OFF state. Once the command register is loaded, the *latching signal* is pulsed low to commit the state of the heater. Therefore, each set/reset command takes less than ten cycles. With a 1-MHz clock signal, the refresh rate is 10^5 heaters/s; thus, a 128-pixel array can be set in < 5 ms. The *asynchronous reset* line, when pulsed low, resets all the heaters in the array to an OFF state. A user interface, written using LabView software (National Instruments, Austin, TX), allows the user to graphically toggle individual heaters in the array and also provides a batch-mode interface in which commands can be read from a text file.

The carrier oil is loaded in a transparent (e.g., glass or plastic) reservoir so that droplet motion can be imaged from below with a charge-coupled-device (CCD) camera. The reservoir

is placed on a glass platform that is actively cooled with a circulating refrigerated water bath (Neslab Endocal). The purpose of the water bath is to prevent heating of the bulk fluid, which can reduce the surface-temperature gradients needed for Marangoni flow and can also cause loss of function or other damage to thermally sensitive samples such as enzymes and other biomolecules. Droplet samples are deposited directly into the oil using a micropipette. The heater array, with the chip resistors facing the oil sample, is then lowered to within 100 μm above the liquid surface using a micromanipulator [Fig. 5(b)]. Prior to the experiment, the glass platform and heater-array board are individually leveled using a bubble tool (i.e., a spirit level). Doing so helps one to keep the heater–liquid separation consistent across the entire array. If desired, droplets can be laterally aligned to the heater array by activating the heaters in a push or a pull mode.

IV. Experimental Results

This section describes experimental results, including the thermal characteristics of the array, experimental flow velocities, droplet velocities in the push and pull modes, and droplet evaporation rates in a one- and two-layer-oil system.

A. Thermal Characterization of the Array

Individual heaters were first tested for thermal efficiency by using a fine-gauge thermocouple (CHAL-0005, Omega Engineering) to measure the temperature as a function of input power. The typical thermal isolation of each heater is ≈120 K/W, and a maximum temperature of 175 °C [Fig. 7(a)] can be achieved without burnout. The thermal time constant of the heater was measured by switching the heater on or off and monitoring its real-time temperature with the thermocouple connected to a data-acquisition card (NI-6062E, National Instruments). When switched on, the heater requires 6.8 s to reach 90% of its maximum temperature. When switched off, it requires 5.6 s to fall to within 10% of the ambient temperature.

Bulk fluid temperatures are kept in check by the circulating water bath. With the cold-water bath being set between 10 °C and 20 °C, the liquid temperature can be maintained under 37 °C. Setting a lower bath temperature results in slower flow velocities due to the increased liquid viscosity at lower temperature.

B. Flow Velocities

Surface-flow velocities were measured by tracking the movement of particles in video clips with frame rates of 30 frames/s. Surface-flow velocities up to 1700 μm/s can be achieved in DC-550 silicone oil and in mineral oil using 1.3-W power at a gap of approximately 300 μm and using 25-μm pollen particles as flow tracers [Fig. 7(b)]. As predicted by simulations, the flow velocity is proportional to the power supplied by the heater. Simulations also predict that the surface-temperature change for achieving 1700-μm/s flow velocity in DC-550 fluid is 24 °C, while the experimentally measured temperature change is between 20 °C and 30 °C. Thus, the simulations and experiments show acceptable agreement. The flow velocity of droplets is small compared to pollen due to their larger mass and drag. A $\Phi = 300$-μm droplet, for example, moves at speeds up to 73 μm/s in the push mode.

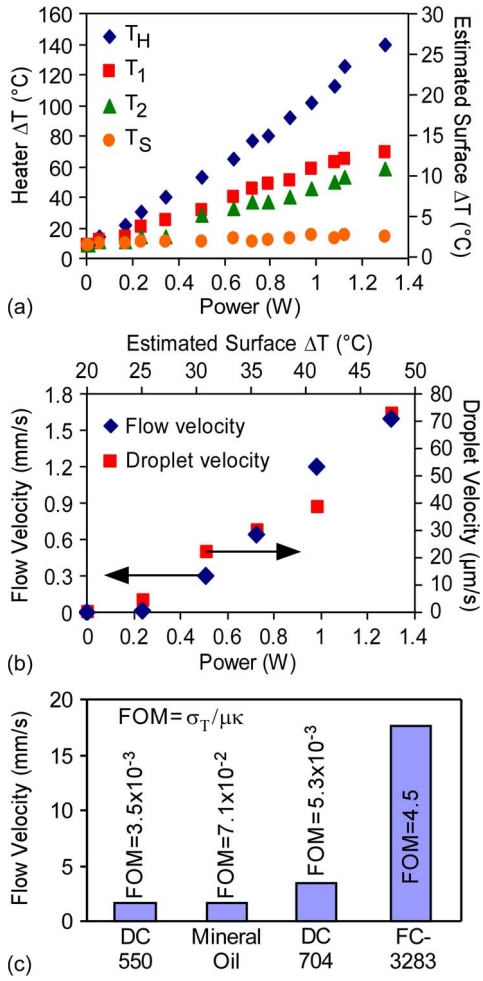

Fig. 7. Experimental results. (a) Temperature of an active heater (T_H) versus input power. Also shown is the temperature increase 1 pixel away (T_1), 2 pixels away (T_2), and, on the substrate, 2 cm away (T_S). (b) Flow velocity (25-μm pollen) and droplet velocity ($\Phi = 300$-μm droplet) versus input power and heater temperature. This experiment used Dow Corning 550 silicone oil and a heater–liquid gap of ~ 300 μm. (c) Comparison of maximum flow velocities obtained with four liquids including mineral oil, Dow Corning 550 and 704 silicone oils, and Fluorinert FC-3283 dielectric liquid. The calculated figures of merit for each fluid are shown in the figure.

In order to obtain faster flow velocities and lower temperature perturbation, alternative fluids with higher figure of merit can be used. Fig. 7(c) compares flow velocities (in the absence of droplets) for four different oils. In three of the four, the flow velocity increases according to the figure of merit. The exception is mineral oil, which appears to have a low velocity for its calculated figure of merit. However, due to the possible variability in various formulations of mineral oil, it is possible that the assumed value of the surface-tension coefficient is not representative of the sample used in the experiment. In particular, it is notable that the reported value [6] is four to ten times higher than those of typical silicone oils. One alternative is Dow Corning 704 fluid, a high-density silicone oil with lower viscosity than DC-550, which helps it attain two times greater flow velocity than that of DC-550 fluid. As mentioned

earlier, fluorinated liquids such as Fluorinert have properties that are well suited for Marangoni-flow generation. Within this family of liquids, FC-3283 is chosen for its low thermal conductivity and low viscosity. The maximum flow velocity measured with FC-3283 was 17 mm/s, which is approximately ten times greater than that of mineral oil and DC-550 fluid at the same power level. Moreover, moderate flow velocities (2.4 mm/s) can be achieved with only 29 mW of input power to the heater, or 1/40th of the power required to achieve the same velocity in DC-550. Thus, FC-3283 is a suitable carrier fluid for obtaining flows with low power and low temperature elevation to the fluid. The compromise is its higher evaporation rate compared to silicone oils.

Another challenge with using FC-3283 is the instability of droplets within the hydrophobic fluid. Aqueous droplets deposited at the center of the fluid reservoir tend to move to the edges of the reservoir where they eventually attach to the reservoir wall. The stabilization problem is solved by adding the fluorous surfactant 1H,1H,2H,2H-perfluoro-1-octanol (PFO, Sigma–Aldrich) to the FC-3283 carrier fluid in a 1: 10 v/v ratio. The surfactant molecules, which are soluble only in the fluorous phase, assemble at the aqueous–fluorous interface and stabilize the droplet [23]. Droplet instability was not observed after adding the surfactant.

C. Push- and Pull-Mode Actuation

Droplets immersed in the carrier fluid can be actuated in either the push or pull mode. Push-mode actuation is most evident in single layers of DC-550 fluid when the droplet's center of gravity is near the surface. This can be ensured in one of two ways: 1) by delivering droplets above the surface of the liquid or 2) by using small droplets ($\Phi < 200$ μm). Experimental observations indicate that, in the former case, the droplet is held above the oil–air interface by interfacial tension. In the latter case (small droplets), the center of gravity is typically near the surface, regardless of how the droplet is dispensed.

In the push mode, surface Marangoni flows drive the droplet away from the active heaters (Fig. 8). Multiheater configurations may be used to direct a droplet in the desired direction. For example, two adjacent heaters activated next to a droplet push the droplet in a straight line, while a right-angle turn can be accomplished using three heaters in an L-shape. In single-layer DC-550 fluid, arbitrary movements at speeds up to 200 μm/s can be generated with sequential activation of such configurations.

In pull-mode actuation, droplets are pulled toward the active heater by subsurface flows. To obtain the pull mode, it is important that the droplet centroid is several hundred micrometers below the surface. To do this, the following conditions should be met: 1) the droplet must be dispensed so that it is submerged beneath the carrier fluid, and 2) the droplet diameter must be larger than 500 μm. Experimental results demonstrate that droplets can be transported at speeds up to 140 μm/s in the pull mode. Compared to the push mode, this mode offers a more scalable control because only a single activated pixel is necessary to trap a droplet. A droplet is initially aligned to a pixel by activating the heater. Subsequently, the sequential activation of adjacent pixels can translate the droplet along a virtual 2-D grid. As a consequence, the pull mode enables the simultaneous actuation and merging of multiple droplets (Fig. 9). Droplet merging, as indicated earlier, is one of the essential functions for droplet-based assays. In this platform, typical droplet volumes are on the order of hundreds of nanoliters.

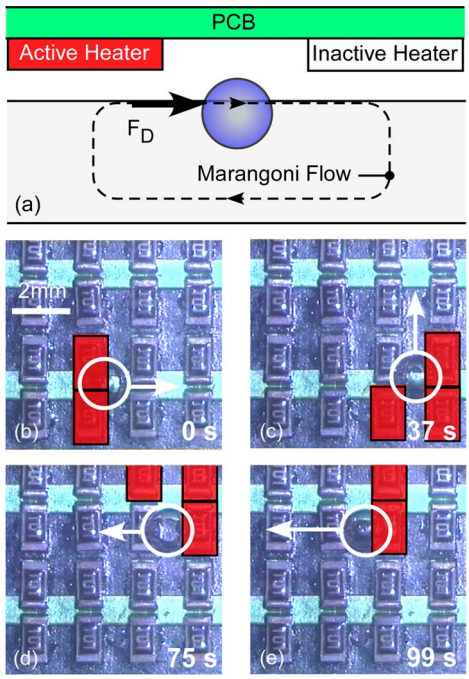

Fig. 8. Push-mode actuation. (a) Surface Marangoni flows create a droplet force (F_D) oriented away from the active heater. (b)–(e) $\Phi = 900$-μm floating droplet is moved along a square path by activating multiheater configurations sequentially. Active heaters are shaded. $P_H = 1$ W/heater, gap ≈ 400 μm, and the fluid is DC-550 silicone oil.

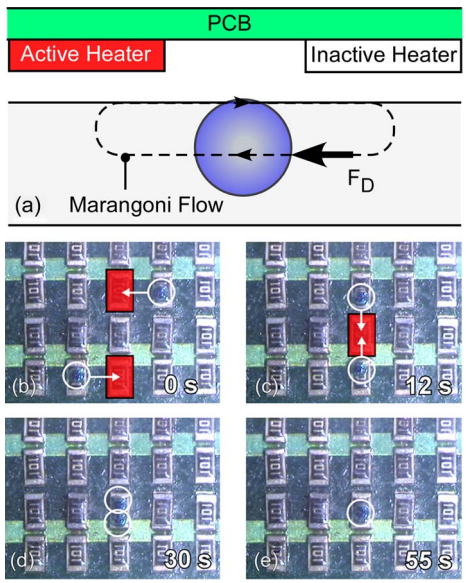

Fig. 9. Pull-mode actuation and droplet merging. (a) Subsurface Marangoni flows create a force on the droplet (F_D) toward the active pixel. (b)–(e) Droplet merging with pull-mode actuation. Two droplets ($\Phi = 600$ μm) are merged through sequential activation of the heaters. Active heaters are shaded. $P_H = 1$ W/heater, gap ≈ 300 μm, and the fluid is DC-550 silicone oil.

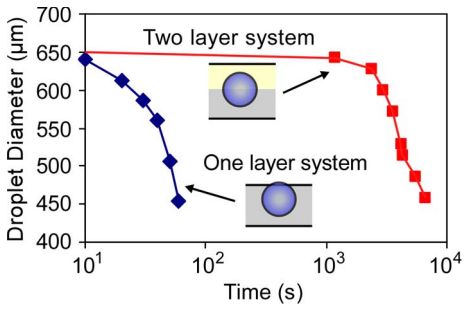

Fig. 10. Preventing droplet evaporation. Measurements showing the variation in droplet size over time (log scale) for a $\Phi = 650$-μm droplet in single- and double-layer-oil systems. The single-layer-oil system consists of DC-550 silicone oil, while the two-layer-oil system consists of DC-550 and mineral oil.

D. Preventing Droplet Evaporation With a Two-Layer-Oil System

When elevated temperatures are used, droplet evaporation can present a challenge. To address this issue, two miscible oils were combined, i.e., one with density that is less than that of water (mineral oil), and the other with density that is greater than water (DC-550 Fluid). In the two-layer system, buoyancy suspends aqueous droplets in between the two layers, unexposed to both air and glass surface below. The suspended droplets are manipulated using subsurface flows (pull-mode actuation). In the two-layer-oil system, evaporation times are on the order of hours, which are 100 times higher than that of the single-layer system where the droplet is exposed (Fig. 10), allowing for assays that require longer incubation times. An added benefit is that it also reduces the overall temperature elevation in the droplet since the majority of temperature perturbation occurs at the liquid surface. The depth of each of the fluid layers plays an important role. In order to achieve pull-mode actuation, it was found that two empirical conditions must be satisfied. First, the diameter of the droplet should be between roughly 500 and 1000 μm. The droplet must be large enough to be pulled toward the heater (see Section II) and small enough to be moved by the Marangoni forces. Second, the thickness of the mineral-oil layer should be more than approximately half the thickness of the DC-550 layer. Since the droplet centroid settles near the interface of the two layers, maintaining a minimum thickness of the mineral-oil layer ensures that the droplet is impacted by subsurface flows directed toward the heater. Under these conditions, the two-layer-oil system enables pull-mode actuation while reducing evaporation by two orders of magnitude.

V. Scaling Analysis and Discussion

It is evident that, as a method for manipulating droplets, Marangoni flows offer the possibility of using blank substrates and the elimination of contact between the actuator and the fluid sample. The overall challenges are efficient energy coupling, lateral heat conduction, increased liquid temperature, and droplet evaporation.

In general, as a surface-dependent phenomenon, the Marangoni effect scales favorably to small length scales when compared to body-force-driven mechanisms. Therefore, the possibility of downscaling the system merits further consideration. To do this, simulation models spanning a large range of length scales were created and analyzed for trends. Both the size of the heater and the gap between the heater and the liquid were varied over two orders of magnitude: The heater radius was scaled from 1 mm to 10 μm, and the gap was correspondingly scaled from 500 to 5 μm while keeping a constant ratio between the radius and the gap. The liquid depth remains constant in order to avoid the increased viscous effects in thin layers. In all of the simulations, the heater power is adjusted in order to obtain a peak temperature change of 10 °C at the surface of the liquid (this is done to compare the effects of downscaling). If a 10-μm heater is used with a 5-μm gap, the temperature gradient is 0.22 K/μm. This is nearly 50 times higher than the gradient achieved at two orders of magnitude larger length scale. Equation (1) suggests that the steeper gradient should result in faster flow velocities at small length scales; however, it is also necessary to consider the increasing viscous forces. The cross-sectional thickness of the flow region decreases with the size of the heat source. For example, at a 30-μm length scale, the flow reverses at a depth of 30 μm, whereas at a 1-mm-length scale, the flow reversal depth is 300 μm. The smaller reversal depth increases the tangential shear forces, which decreases surface velocities. As a result, the Marangoni-flow velocities do not improve at length scales below about 100 μm. From this study, it is concluded that 100-μm heaters are an appropriate size scale for near-maximum efficiency. It should also be noted that the range of droplets that can be trapped depends on the flow reversal depth. At a 100-μm scale, with a flow reversal depth of 80 μm, it is estimated that 80–100-μm diameter (270–520 pL) can be efficiently actuated in the pull mode. Overall, scaling to smaller dimensions results in the following: 1) decreased power consumption; 2) increased velocity (as long as the length scale is > 100 μm); and 3) the ability to manipulate smaller droplets.

Miniaturization and scaling to large arrays is not without challenges. For example, miniaturization may offer lower power consumption per heater, but the larger number of heaters in a high-density device would increase the overall system power consumption. Thermal crosstalk between heaters must also be considered when placing heaters at a smaller pitch. Issues such as these will require the careful design of a high-density array and appropriate heat sinking in order to deliver efficient isolated temperature perturbations on the liquid surface.

An alternate way to improve efficiency is to place the heat sources as close to the surface as possible. This increases not only the coupling ratio $(\Delta T_{\mathrm{Surface}}/\Delta T_{\mathrm{Heater}})$ but also the lateral temperature gradient that is necessary for producing flow. With an array of heaters, the challenge is to keep the heater–liquid separation small and equal for all of the heaters in the array. The present approach can obtain gaps as low as 100–200 μm; but this can be improved by using optical or other servo control systems for more precise positioning and leveling.

Finally, one must increase the efficiency of the heater itself. Microfabricated devices with thermally insulative materials and small cross sections can provide high efficiency and fast time constants. For example, a polyimide cantilever with an integrated heater can achieve 100-°C temperature while dissipating

only 10 mW of applied power [24]. Such heaters would reduce power consumption by up to two orders of magnitude, which is important, particularly if the number and density of the heaters in the array are scaled up.

In order to allow localized control, thermal crosstalk between heaters should be considered. The present experiments show a crosstalk ratio of 30% between adjacent pixels (Fig. 7) due to parasitic heat flow through the PCB board. Improvements can be made by a number of means, such as using a thinner PCB board, removing portions of the board to decrease conduction, or by placing a thermally insulative barrier between the heaters and the PCB (while maintaining electrical conductivity).

Overall, compared to other droplet manipulation techniques, the primary advantages offered by the use of Marangoni flows are as follows: 1) It requires no interaction between the droplet and the substrate, thus circumventing potential issues of contamination, and 2) it can be used on substrates that do not have complex structures (or even channels) for handling liquids. However, as a thermal technique, the parasitic heating of the liquid is a drawback. The use of suspended heat sources is important because it reduces the heat transferred to the liquid while simultaneously allowing a high-temperature gradient to be achieved. A microfabricated heater array can potentially achieve superior temperature gradients. The results of this paper highlight the importance of a carrier fluid that provides a high surface-tension temperature coefficient. Areas of potential future work include the following. First is increasing the speed of droplet manipulation. By choosing optimal liquids with low viscosities and thermal conductivities, it may be possible to achieve further gains in droplet speed. Optimization of the relative viscosities of oil and water may affect the performance of droplet merging and can be further investigated. Second is performing other droplet operations. Droplet metering and splitting operations that are necessary for generalized assays can be investigated by either using Marangoni flows or combining this method with existing approaches. Third is further miniaturization. Simulations predict that miniaturization will facilitate manipulation of smaller droplets with less power and temperature requirements.

VI. Conclusion

This paper has explored how Marangoni flows can be deliberately controlled by creating dynamic temperature profiles on the liquid surface. A contactless programmable droplet manipulation system that utilizes the Marangoni effect has been demonstrated. The distinguishing feature of the approach is that the suspended droplets can be controlled without contact with solid surfaces and that the substrate can remain blank and featureless. Programmable manipulation and merging of multiple droplets were demonstrated using a system with 128 heaters and a software-controlled interface. One of the challenges of the technique, particularly for biomedical assays, is the temperature change required in the liquid. Initial experiments using common silicone oils indicate a 20–30-°C temperature elevation. However, it was shown that the temperature change and power consumption can be reduced by a factor of 40 by using a fluid such as Fluorinert that has a high figure of merit. Scaling to smaller sizes does not increase flow speeds; however, it reduces power consumption and allows digital control of smaller droplets. The future direction of this paper is to develop a microfabricated heater array that will achieve these performance improvements and also allow high-throughput manipulation of a larger number of droplets.

References

[1] P. Gravesen, J. Branebjerg, and O. S. Jensen, "Microfluidics—A review," *J. Micromech. Microeng.*, vol. 3, no. 4, pp. 168–182, Dec. 1993.

[2] T. Squires and S. R. Quake, "Microfluidics: Fluid physics at the nanoliter scale," *Rev. Mod. Phys.*, vol. 77, no. 3, pp. 977–1026, Jul. 2005.

[3] S. K. Cho, H. Moon, and C.-J. Kim, "Creating, transporting, cutting, and merging liquid droplets by electrowetting-based actuation for digital microfluidic circuits," *J. Microelectromech. Syst.*, vol. 12, no. 1, pp. 70–80, Feb. 2003.

[4] S. Zeng, C.-H. Chen, J. C. Mikkelsen, Jr., and J. G. Santiago, "Fabrication and characterization of electroosmotic micropumps," *Sens. Actuators B, Chem.*, vol. 79, no. 2/3, pp. 107–114, Oct. 2001.

[5] M. K. Chaudhury and G. M. Whitesides, "How to make water run uphill," *Science*, vol. 256, no. 5063, pp. 1539–1541, Jun. 1992.

[6] T. S. Sammarco, "A microfluidic thermocapillary pumping system for microfabricated analysis devices," Ph.D. dissertation, Univ. Michigan, Ann Arbor, MI, 1999.

[7] A. A. Darhuber, J. P. Valentino, J. M. Davis, S. M. Troian, and S. Wagner, "Microfluidic actuation by modulation of surface stresses," *Appl. Phys. Lett.*, vol. 82, no. 4, pp. 657–659, Jan. 2003.

[8] A. D. Stroock, R. F. Ismagilov, H. A. Stone, and G. M. Whitesides, "Fluidic ratchet based on Marangoni–Benard convection," *Langmuir*, vol. 19, no. 10, pp. 4358–4362, May 2003.

[9] A. S. Basu and Y. B. Gianchandani, "Shaping high-speed Marangoni flow in liquid films by microscale perturbations in surface temperature," *Appl. Phys. Lett.*, vol. 90, no. 3, pp. 034 102-1–034 102-3, Jan. 2007.

[10] A. S. Basu and Y. B. Gianchandani, "Virtual microfluidic traps, filters, channels, and pumps using Marangoni flows," *J. Micromech. Microeng.*, vol. 18, no. 11, p. 115 031, Nov. 2008.

[11] A. S. Basu, "Microthermal devices for fluidic actuation by modulation of surface tension," Ph.D. dissertation, Univ. Michigan, Ann Arbor, MI, Aug. 2008.

[12] A. S. Basu and Y. B. Gianchandani, "A 128-pixel digitally programmable microfluidic platform for non-contact droplet actuation using Marangoni flows," in *Proc. Int. Conf. Solid State Sens., Actuators, Microsyst. (Transducers)*, Lyon, France, Jun. 2007, pp. 771–774.

[13] H. Song, J. D. Tice, and R. F. Ismagilov, "Reactions in droplets in microfluidic channels," *Angew. Chem. Int. Ed.*, vol. 42, pp. 768–772, 2003.

[14] P. R. C. Gascoyne, J. V. Vykoukal, J. A. Schwartz, T. J. Anderson, D. M. Vykoukal, K. W. Current, C. McConaghy, F. F. Becker, and C. Andrews, "Dielectrophoresis-based programmable fluidic processors," *Lab Chip*, vol. 4, no. 4, pp. 299–309, Aug. 2004.

[15] V. Srinivasan, V. K. Pamula, and R. B. Fair, "An integrated digital microfluidic lab-on-a-chip for clinical diagnostics on human physiological fluids," *Lab Chip*, vol. 4, no. 4, pp. 310–315, Aug. 2004.

[16] P. Y. Chiou, H. Moon, H. Toshiyoshi, C.-J. Kim, and M. C. Wu, "Light actuation of liquid by optoelectrowetting," *Sens. Actuators A, Phys.*, vol. 104, no. 3, pp. 222–228, May 2003.

[17] A. Rida, V. Fernandez, and M. A. Gijs, "Long-range transport of magnetic microbeads using simple planar coils placed in a uniform magnetostatic field," *Appl. Phys. Lett.*, vol. 83, no. 12, pp. 2396–2398, Sep. 2003.

[18] S. K. Sia and G. M. Whitesides, "Microfluidic devices fabricated in poly(dimethylsiloxane) for biological studies," *Electrophoresis*, vol. 24, no. 21, pp. 3563–3576, Nov. 2003.

[19] J.-Y. Yoon and R. L. Garrell, "Preventing biomolecular adsorption in electrowetting-based biofluidic chips," *Anal. Chem.*, vol. 75, no. 19, pp. 5097–5102, 2003.

[20] F. J. Higuera, "Steady thermocapillary-buoyant flow in an unbounded liquid layer heated nonuniformly from above," *Phys. Fluids*, vol. 12, no. 9, pp. 2186–2197, Sep. 2000.

[21] R. Eötvös, "Ueber den zusammenhang der oberflächenspannung der flüssigkeiten mit ihrem molecularvolumen," *Ann. Phys.*, vol. 263, no. 3, pp. 448–459, 1886.

[22] S. R. Palit, "Thermodynamic interpretation of the Eötvös constant," *Nature*, vol. 177, no. 4521, p. 1180, Jun. 1956.

[23] L. S. Roach, H. Song, and R. F. Ismagilov, "Controlling nonspecific protein adsorption in a plug-based microfluidic system by controlling

interfacial chemistry using fluorous-phase surfactants," *Anal. Chem.*, vol. 77, no. 3, pp. 785–796, Feb. 2005.
[24] M. H. Li and Y. B. Gianchandani, "Applications of a low contact force polyimide shank bolometer probe for chemical and biological diagnostics," *Sens. Actuators A, Phys.*, vol. 104, no. 3, pp. 236–245, May 2003.
[25] *Fluorinert Electronic Liquid FC-3283*, 3M Specialty Mater., St. Paul, MN, 2001.
[26] Y. Bertrand and L. C. Hoang, "Vegetal oils as substitute for mineral oils," in *Proc. 7th Int. Conf. Properties Appl. Dielectr. Mater.*, Nagoya, Japan, Jun. 2003, pp. 491–494.
[27] *Information About Dow Corning 510, 550, 710 Fluids*, Dow Corning Corporation, Midland, MI, 1998.
[28] *Information About Dow Corning 704 Diffusion Pump Fluid*, Dow Corning Corporation, Midland, MI, 1998.
[29] M. A. McClain, C. T. Culbertson, S. C. Jacobson, N. L. Allbritton, C. E. Sims, and J. M. Ramsey, "Microfluidic devices for the high-throughput chemical analysis of cells," *Anal. Chem.*, vol. 75, no. 21, pp. 5646–5655, Nov. 2003.
[30] S. J. VanHook, M. F. Schatz, J. B. Swift, W. D. McCormick, and H. L. Swinney, "Long-wavelength surface-tension-driven Benard convection: Experiment and theory," *J. Fluid Mech.*, vol. 345, pp. 45–78, 1997.

Amar S. Basu received the B.S.E. and M.S.E. degrees in electrical engineering in 2001 and 2003, respectively, the M.S. degree in biomedical engineering in 2005, and the Ph.D. degree in electrical engineering in 2008, all with honors, from the University of Michigan, Ann Arbor.

He worked with Intel's Advanced Technology Division, General Motors, and Silicon Graphics, and served as an adjunct faculty member in the Department of Electrical Engineering, University of Michigan. Currently, he is an Assistant Professor in the Department of Electrical and Computer Engineering, Wayne State University, Detroit, MI. His research interests include the development of micro and nanoscale systems for high throughput screening and other areas of biological research.

Dr. Basu was a recipient of the Whitaker Foundation Biomedical Engineering Fellowship, and was voted the IEEE Professor of the Year by the student body in 2009. His work as a consultant with Mobius Microsystems and Picocal has resulted in a number of U.S. patents.

Yogesh B. Gianchandani received a B.S., M.S., a Ph.D. in electrical engineering, with a focus on microelectronics and MEMS. He is presently a Professor at the University of Michigan, Ann Arbor, with a primary appointment in the Electrical Engineering and Computer Science Department and a courtesy appointment in the Mechanical Engineering Department. He is temporarily serving at the National Science Foundation, as the program director within the Electrical, Communication, and Cyber Systems Division (ECCS).

Dr. Gianchandani's research interests include all aspects of design, fabrication, and packaging of micromachined sensors and actuators and their interface circuits (http://www.eecs.umich.edu/~yogesh/). He has published approximately 200 papers in journals and conferences, and has about 30 U.S. patents issued or pending. He was a Chief Co-Editor of *Comprehensive Microsystems: Fundamentals, Technology, and Applications*, published in 2008. He serves several journals as an editor or a member of the editorial board, and served as a General Co-Chair for the IEEE/ASME International Conference on Micro Electro Mechanical Systems (MEMS) in 2002.